ELSEVIER

Contents lists available at ScienceDirect

# Aquaculture

journal homepage: www.elsevier.com/locate/aquaculture





# Multi-omics reveals the molecular mechanisms of rapid growth in distant hybrid fish

Xuanyi Zhang, Fanglei Liu, Bei Li, Lujiao Duan, Jianming Yu, Ziyi Huang, SiYang Huang, Hongwen Liu, Qingfeng Liu, Shaojun Liu

State Key Laboratory of Developmental Biology of Freshwater Fish, Engineering Research Center of Polyploid Fish Reproduction and Breeding of the State Education Ministry, College of Life Sciences, Hunan Normal University, Changsha 410081, Hunan, PR China

ARTICLE INFO

Keywords: Distant hybridization Growth Gut microbiota Multi-omics analysis

#### ABSTRACT

Distant hybridization usually results in heterosis. In previous studies, we obtained an improved fish (WR-II, 2n = 100) with rapid growth through distant hybridization. To investigate the molecular mechanisms underlying the rapid growth of WR-II, the intestinal structure, microbiome and metabolome of the gut and the transcriptome of muscle were compared between WR-II and its parents (WCC and RCC, 2n = 100). The results revealed that WR-II had more intestinal folds, and the height, width and goblet cell density of the intestinal folds were greater than those of its parents. The absolute abundances of the probiotics Ralstonia and Salinivibrio were significantly greater in WR-II than in the parents (p < 0.05), and the probiotic *Cupriavidus* was found in only WR-II. A total of 481 and 718 differentially abundant metabolites (DMs) were identified in WR-II vs. WCC and WR-II vs. RCC, respectively. These DMs were enriched mainly in pathways related to metabolism, protein synthesis and development, such as fumaric acid, sphingosine, betaine and 5'-adenylic acid (AMP). A total of 5680 and 11,795 differentially expressed genes (DEGs) were identified in WR-II vs. WCC and WR-II vs. RCC, respectively. These DEGs were enriched mainly in pathways related to protein synthesis and substance metabolism. Growth-related genes such as irs1, irs2, foxo1, igf1r, and akt were upregulated in WR-II. Multi-omics analysis revealed that Salinivibrio can promote the level of AMP, which then regulates the expression of irs1 and foxo1, thus promoting the growth of WR-II. This study revealed the mechanism of rapid growth of WR-II from the probiotics, metabolites and genes, which provides evidence for the molecular mechanism of heterosis.

#### 1. Introduction

The practice of aquaculture is important in addressing the dual challenges of declining fish stocks in natural waters and the growing demand for fish products (Blanchard et al., 2017; Hu et al., 2021). Currently, most farmed fish take a long time to reach a commercially viable size, so it is particularly important to breed new varieties of aquatic animals that grow quickly. Distant hybridization is widely used in fish genetic breeding, as it integrates the genomes of both parents, leading to changes in the genotype and phenotype of the offspring (Liu et al., 2018; Liu, 2010; Liu et al., 2016). The offspring of hybrids usually exhibit heterosis, particularly in terms of improved growth rates and increased resistance to disease (Guo et al., 2018; Li et al., 2022). Currently, many hybrid fish with good growth performance are widely used in aquaculture and have considerable economic benefits (Gong et al., 2022; Gong et al., 2021; Liu et al., 2019; Wang et al., 2020).

Several factors influence fish growth, and research on the regulatory mechanisms of hybrid fish growth has focused mainly on molecular mechanisms (Xu et al., 2019), hormone levels (Fuentes et al., 2013), and environmental factors (Reinecke, 2010). However, studies on the role of the gut in fish growth performance remain relatively rare.

The gut is the largest surface of fish that faces the external environment (Schug et al., 2019). It is in direct contact with symbiotic microorganisms and nutrients in the diet and plays an important role in the digestion and absorption of substances and the promotion of host growth (Chen et al., 2023; Su et al., 2021b). Research has demonstrated that intestinal folds significantly enhance the surface area, thereby facilitating the digestion and absorption of nutrients. Furthermore, the number of folds is positively associated with the quantity of intestinal epithelial cells. An increase in the number of folds correlates with improved digestive and absorptive capacity (Li et al., 2013; Morrison and Wright, 1999). In recent years, it has become evident that the gut

E-mail addresses: Liuqingfeng@hunnu.edu.cn (Q. Liu), lsj@hunnu.edu.cn (S. Liu).

<sup>\*</sup> Corresponding authors.

microbiota is essential for host growth, development, and reproduction (Chen et al., 2023; Lozupone et al., 2012). Fish are exposed to millions of microorganisms in water, and the composition of the gut microbiota can vary greatly between species (Larsen, 2014; Minich et al., 2020). Furthermore, the gut microbiota primarily utilize dietary substrates that are not digested by enzymes, as well as endogenous secretions, to synthesize various metabolites (Rohr et al., 2020; Roques et al., 2020). Research has shown that microbial metabolites, such as short-chain fatty acids (SCFAs), phenolic compounds, bile acids, and conjugated linoleic acid, can improve muscle glucose homeostasis, energy expenditure, protein synthesis, and physiological functions by regulating gut permeability and directly or indirectly targeting skeletal muscle (Neis et al., 2015; Rowland et al., 2018). Many studies have confirmed the existence of the gut-brain axis, gut-liver axis, and gut-skin axis in fish (Fu et al., 2024; Liu et al., 2024; Polakof et al., 2011). The functionality of these pathways is related to the regulation of energy metabolism by the gut microbiota (Ma et al., 2020; Ma and Ma, 2019). Additionally, there is sufficient evidence to support the existence of the gut-muscle axis, although related research in fish is still limited (Grosicki et al., 2018). Lahiri et al. reported that germ-free mice presented a certain degree of skeletal muscle atrophy, with decreased expression of genes and proteins associated with skeletal muscle growth, mitochondrial function, and muscle-neuron signaling (Lahiri et al., 2019). The continuous feeding of exogenous short-chain fatty acids partially reversed muscle damage in germ-free mice, indicating that the microbiota and their metabolites play important roles in the gut-muscle axis (Okamoto et al., 2019). Research on pigs has shown that antibiotic treatment alters the gut microbiota composition, positively affecting growth performance, thus suggesting that gut microbiota could be a potential target for regulating host skeletal muscle characteristics (Yan et al., 2020). Additionally, studies in humans have indicated that the proportion of skeletal muscle fiber types is also regulated by the gut microbiota (Grosicki et al., 2018). In recent years, the importance of research on fish gut microbiota has become increasingly evident, highlighting its potential to advance the aquaculture industry and making it a hot topic and frontier of research.

Single-omics data are insufficient for comprehensively analyzing the regulatory mechanisms of complex physiological processes. In contrast, Multi-omics integration analysis can be used to explore potential regulatory networks within organisms, providing more robust evidence for understanding biological mechanisms (Zhang et al., 2010). The interaction mechanisms between the gut microbiota, their metabolites, and host growth performance are not yet fully understood. Recently, integrated omics analysis has offered new perspectives for studying the diverse gut microenvironments in fish. For example, by combining microbiome and metabolome data, Sparagon et al. discovered that the gut microbiota and metabolites of herbivorous fishes continuously covary and differentiate from the stomach to the hindgut (Sparagon et al., 2022). By integrating metabolome and transcriptome data, Li et al. reported that changes in fish gut metabolites under cold stress are closely related to various metabolic and immune pathways (Li et al., 2024). Combining microbiome and transcriptome data, Su et al. revealed that the gut microbial structure of a new strain of carp affects its growth performance by regulating gut gene expression (Su et al., 2021a). In previous studies, we obtained an improved crucian carp (WR-II, 2n = 100) through distant hybridization, and WR-II exhibited significantly faster growth than its parents (Carassius cuvieri, WCC, and Carassius auratus red var., RCC) (Liu et al., 2019). This study employed 16S rRNA gene sequencing, LC-MS metabolomics, and transcriptomics to conduct a longitudinal multi-omics integration analysis. We aimed to investigate the regulatory mechanism of rapid growth of WR-II in terms of gut microbes, metabolites and genes, providing evidence for the molecular mechanisms underlying heterosis through distant hybridization.

#### 2. Materials and methods

#### 2.1. Ethics statement

The fish used in this study are non-rare and non-endangered fish (not classified as national first or second class protected animals). Researchers have certification from Hunan Normal University's professional training course for animal laboratory practitioners. Prior to dissection, all fish were anaesthetized deeply using 80 mg/L MS-222 for humanitarian treatment.

#### 2.2. Sample collecting

The fish (WR-II, WCC, and RCC) were cultivated at the Engineering Research Center of Polyploid Fish Breeding and Reproduction of the State Education Ministry, Hunan Normal University. WCC and RCC classified into different species in the genus of Carassius (Liu et al., 2019). The breeding strategy of the experimental fish was shown in Fig. S1, and the specific methods refer to previous studies (Wang et al., 2015; Liu et al., 2019). A total of 50 fish (eight-month-old) were selected randomly from each group for light anesthesia, weighing and recording. The mean weights of the WR-II, WCC, and RCC groups were 427.1  $\pm$ 19.3 g,  $276.1 \pm 12.2$  g, and  $252.6 \pm 10.6$  g, respectively. The health of the fish was ensured prior to sampling. Following a 24-h period of fasting, the abdomen was dissected with sterile dissecting scissors, the intestines were removed, and the intestine was rinsed with 0.9 % sterile saline under aseptic conditions. A segment of the mid-intestine was excised, the ends of the intestines were cut open, and the contents were collected with a sterile surgical blade for 16S rRNA gene sequencing and metabolite detection. Muscle samples were taken by removing the scales from the back and excising the dorsal muscle. Samples were aliquoted and labeled in RNase-free EP tubes, quickly taken (within 5-10 min) for transcriptome sequencing, and snap frozen immediately in liquid nitrogen at −80 °C.

#### 2.3. Intestinal structure

A total of six fish of each of WR-II, WCC and RCC were randomly selected for euthanasia. The abdomen was incised with dissecting scissors, and the intestines were subsequently removed. The midgut was then amputated and fixed in a paraformaldehyde solution for 24 h. Subsequently, the intestines were dehydrated in an ethanol gradient series, followed by clearing with xylene, dipping in wax, and embedding the intestinal tissue in paraffin. The tissues were sectioned at a thickness of 5  $\mu m$  using a sectioning machine, stained with hematoxylin and eosin (HE), prepared as histological paraffin sections, and finally observed and photographed (Cinar and Şenol, 2006). The height and width of 10 intestinal villi and the thickness of the muscularis propria were measured in each section, with the average value taken as the measurement value. The number of goblet cells was counted in three randomly photographed non-overlapping fields of view, with the mean value taken as the final number of goblet cells.

## 2.4. 16S rRNA gene sequencing

This project involved the 16S rRNA gene sequencing and analysis of six intestinal content samples from each experimental fish to detect the composition and abundance of intestinal microbiota. Firstly, total genomic DNA was extracted from the intestinal contents, and the concentration and purity of DNA were analyzed on a 1 % agarose gel using the NanoDrop 2000 spectrophotometer (Thermo Fisher, USA). The V3 and V4 hypervariable regions (400–450 bp) of the bacterial 16S rRNA gene were amplified using the universal PCR primers 515F [5' –GTGCCAGCMGCCGCGG TAA–3'] and 806R [5' –GGACTACHVGGGTWTCTAAT–3']. Detailed experimental procedures are described in other studies (Bokulich et al., 2013). Microbial diversity

analysis was conducted using QIIME 2 software, and  $\alpha$  and  $\beta$  diversity indices were calculated (Wang et al., 2021).

#### 2.5. LC-MS

A metabolomic study was conducted using non-targeted liquid chromatography-mass spectrometry (LC-MS) on six intestinal content samples from each experimental fish, with the objective of analyzing the types and differences in metabolites present in the intestine. To extract the metabolites, 100 mg of each intestinal content sample was subjected to homogenization, and the resulting supernatant (250 uL per sample) was subsequently collected. The LC-MS analysis experimental steps and instrumental procedures are detailed in previous studies (Zhan et al., 2022). The chromatographic gradient elution program followed a previously described method (Want et al., 2013). Positive and negative ions were combined and analyzed, the raw data files (.raw) were processed using CD3.3 software. Metabolite identification and relative quantification were performed using the mzCloud, mzVault, and Masslist databases. We screened for differential metabolites based on the criteria VIP > 1.0, FC > 1.5 or FC < 0.667 and P < 0.05. The KEGG, HMDB, and LIPID Maps databases were used to identify metabolites.

#### 2.6. Transcriptome sequencing and analysis

Three fish from each of WR-II, WCC and RCC were selected randomly for the transcriptome analysis (a total of 12 samples). Total RNA was extracted from muscle tissue using the RNA kit (Omega, USA). We quantified the integrity and quality of RNA using capillary electrophoresis (Bioanalyzer, Agilent Technologies) to ensure it adhered to the sequencing requirements. Subsequently, RNA libraries were constructed using the RNA Library Preparation Kit (New England Biolabs). This process included reverse transcription of RNA, ligation of sequencing adapters, and PCR amplification. The constructed libraries were then subjected to quality checks again using the Bioanalyzer to ensure they met the expected quality standards. For quality control (QC), lowquality sequences were removed, adaptor sequences were filtered out, and PCR duplicates were eliminated. The sequences were aligned to the reference transcriptome. DEGs were calculated with the DeSeq2 package in R software, with a screening threshold of  $|\log_2(\text{fold change})| > 1$  and padj <0.01 from the WR-II vs. WCC and WR-II vs. RCC comparisons. DEGs were analyzed for functional enrichment and pathway analysis, and sequence annotations were performed using the protein database (NCBI). GO functional classification and KEGG pathway analysis were conducted using cluster Profiler.

## 2.7. Multi-omics analysis

All DEGs and DMs were mapped to the Kyoto Encyclopedia of Genes and Genomes (KEGG) pathway database to obtain information regarding the common pathway and to identify the principal biochemical and signal transduction pathways in which the DEGs and DMs are involved (Supplementary materials 2). Pearson correlation analysis was used to screen for DEGs and DMs according to the targeted growth-related pathways, in order to identify DEGs and DMs with significant correlations. Pearson correlation analysis was then conducted between the significantly different probiotic genera obtained from 16S rDNA analysis and growth-related metabolites to assess the relationship between microbial species diversity and metabolites. The probiotic genera, DMs and DEGs expression data required for mapping are shown in Table S2.

# 2.8. Validation of significant DEGs by RT-qPCR

Total RNA was extracted from muscle tissues and first-strand cDNA was obtained by reverse transcription kit (Thermo Fisher Scientific, USA). The primers were synthesized by Sangon Biotech (Shanghai,

China), and their sequences are provided in Table S3.  $\beta$ -actin was used as a control. The mRNA expression levels were determined using PowerUp<sup>TM</sup> SYBR<sup>TM</sup> Green Master Mix (Thermo Fisher Scientific, USA) on Quant Studio 5 system (Life Technologies, USA). The relative expression level was calculated using the  $2^{(-\Delta\Delta CT)}$  method.

#### 2.9. Statistical analysis

All statistics are presented as mean  $\pm$  standard error (SE). Student's t-test was performed for data analysis using SPSS 26 statistical software. Statistical analyses were performed and plotted using GraphPad Prism 10. Pearson correlation coefficients were used to analyze correlations between multi-omics data. Advanced Cor link was performed using the OmicStudio tools at <a href="https://www.omicstudio.cn/tool">https://www.omicstudio.cn/tool</a>. P < 0.05 was considered statistically significant.

## 3. Results

#### 3.1. Intestinal morphology

The intestinal structures of WR-II, WCC and RCC are shown in Fig. 1. The intestinal mucosa (M), submucosa layer (SM), muscle layer (ML), and serous membrane (S) structures are clearly visible. Goblet cells (GCs) were distributed among the absorptive cells of the intestinal folds (Fig. 1D, E, F). In addition, we measured and analyzed various morphological features of the intestines (Table 1). The number of intestinal folds in WR-II (19-21) was greater than that in WCC (16-18) and RCC (16–18). The fold height (hF) in WR-II (235.52  $\pm$  17.42  $\mu$ m) was significantly greater than that in RCC (124.39  $\pm$  11.37  $\mu m$ ) and WCC  $(207.25 \pm 15.79 \,\mu\text{m}) \, (p < 0.05)$ . The fold width (wF) in WR-II (71.45  $\pm$ 3.55 µm) was significantly greater than that in RCC (39.62  $\pm$  2.89 µm) and WCC (50.12  $\pm$  5.48  $\mu$ m) (p < 0.05). The muscle thickness (tML) in WR-II (41.47  $\pm$  2.35  $\mu m)$  was also greater than that in RCC (36.11  $\pm$ 0.93  $\mu m)$  and WCC (36.98  $\pm$  1.41  $\mu m). Moreover, the goblet cell density$ in WR-II (633.93  $\pm$  17.99 cells/mm<sup>2</sup>) was significantly greater than that in RCC (587.06  $\pm$  8.26 cells/mm<sup>2</sup>) and WCC (602.15  $\pm$  9.53 cells/mm<sup>2</sup>) (p < 0.05).

#### 3.2. Gut microbial community and probiotic levels

We sequenced the 16S rDNA V3-V4 variable region of the gut contents of WR-II and its parents, to analyze the composition and differences in gut microbiota among the three fish. A total of 1884 operational taxonomic units (OTUs) were detected. All 1884 OTUs (100 %) were annotated in the database, with annotation rates at the domain, phylum, class, order, family, genus, and species levels of 100 %, 99.79 %, 99.58 %, 97.98 %, 95.17 %, 82.32 %, and 45.70 %, respectively. The results of the microbiome alpha diversity analysis are shown in Table 2. The Good's coverage values were all 1, indicating high microbial detection coverage and that the sequencing results accurately represented the samples. PCoA and UPGMA clustering analysis (Weighted unifrac distance) revealed distinct separations between WR-II and WCC and RCC (Fig. 2A, B).

Additionally, the microbial abundance (absolute abundance) of the fish differed under the same rearing conditions. At the phylum level, Bacteroidota, Proteobacteria, Firmicutes, and Chloroflexi were the dominant phyla in the intestines of the fish, accounting for more than 90 % of the total abundance. Bacteroidetes was the dominant phylum in WR-II with a high abundance (59.92 %), whereas Proteobacteria was the dominant phylum in WCC and RCC (41.44 % and 52.91 %, respectively) (Fig. 2C). At the genus level, we identified the top 10 probiotic genera in the gut microbiota of WR-II, ranked by absolute abundance: *Ralstonia, Salinivibrio, Bacteroides, Cetobacterium, Deinococcus, Exiguobacterium, Faecalibacterium, Parasutterella, Cupriavidus*, and *Coprococcus*. We compared these probiotic genera between WR-II and WCC, and between WR-II and RCC (Fig. 2D). In the WR-II and WCC comparisons, the

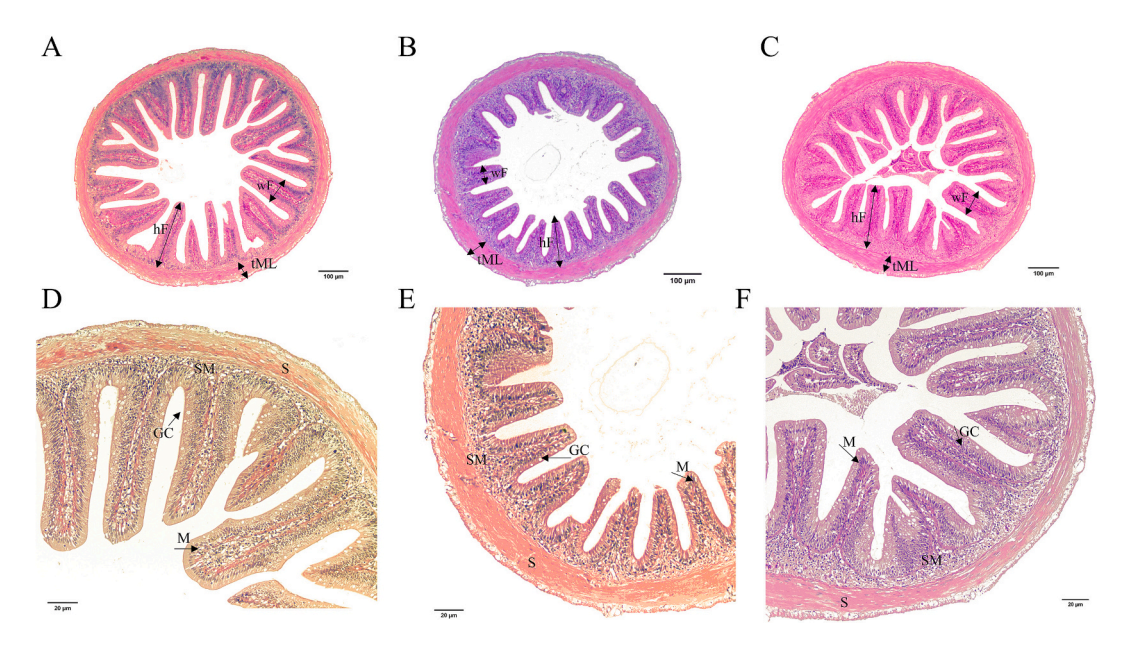


Fig. 1. Morphology of the intestines of WR-II, WCC, and RCC. (A, D) WR-II, (B, E) WCC, and (C, F) RCC. SM: submucosal layer; M: mucosa; S: serous membrane; GC: goblet cells; wF: fold width; hF: fold height; tML: muscle thickness. A, B, C Scale bars = 100 μm, D, E, F Scale bars = 20 μm.

**Table 1** Indicators of gut morphology in WR-II, WCC and RCC.

Group	Intestinal fold	Fold height (µm)	Fold width (µm)	Muscle thickness (μm)	Goblet cell density (cell/mm²)
WCC	16–18	$207.25 \pm \\ 15.79^{ac}$	$50.12 \pm \\5.48^{ac}$	$36.98 \pm \\1.41$	$602.15 \pm 9.53^{a}$
RCC	16–18	$124.39 \pm \\11.37^{ab}$	$\begin{array}{c} 39.62 \pm \\ 2.89^{ab} \end{array}$	$36.11 \pm 0.93$	$587.06 \pm 8.26^{a}$
WR-II	19–21	$235.52 \pm \\ 17.42^{bc}$	$71.45 \pm 3.55^{bc}$	$41.47 \pm \\2.35$	$633.93 \pm \\17.99^{bc}$

Note: Values are means  $\pm$  SE, n=6. a indicates that it was significant differences with WR-II (p<0.05).

b indicates significant difference with WCC (p < 0.05). c indicates significant difference with RCC (p < 0.05).

absolute abundances of *Ralstonia*, *Salinivibrio*, *Bacteroides*, *Exiguobacterium*, and *Faecalibacterium* were significantly greater in WR-II comparison (p < 0.05). However, *Deinococcus*, *Parasutterella*, *Cupriavidus*, and *Coprococcus* were absent in WCC and unique to WR-II. In the WR-II and RCC comparison, the abundances of *Ralstonia*, *Salinivibrio*, and *Coprococcus* were significantly greater in the WR-II comparison (p < 0.05). Similarly, *Cupriavidus* was also unique to WR-II. Overall, the abundances of *Ralstonia* and *Salinivibrio* in WR-II were significantly greater than those in the parents, and Cupriavidus was unique to WR-II.

# 3.3. Intestinal metabolite analysis

Nontargeted metabolomics (LC–MS) was used to determine the metabolic profiles of the intestinal contents of WR-II, WCC, and RCC. Metabolomic data clearly distinguished WR-II from WCC and RCC in the PCA and OPLS-DA models, laying the foundation for subsequent

differentially abundant metabolite screening. The clustering heatmap (Fig. 3B) revealed that samples within groups clustered closely, whereas the intergroup distances were relatively large (Fig. 3B). A total of 1979 metabolites were identified in 18 samples from WR-II, WCC, and RCC. A total of 481 metabolites were significantly different between WR-II and WCC, with 406 upregulated and 75 downregulated (Fig. 3C). A total of 718 metabolites were significantly different between WR-II and RCC, with 547 upregulated and 171 downregulated (Fig. 3D). HMDB classification indicated that the DMs were mainly lipids and lipid-like molecules, organic acids and derivatives, and organic heterocyclic compounds (Fig. 3E).

The DMs were annotated to KEGG pathways. The top 20 enriched pathways for DMs in the two comparison groups are shown in Fig. 3. Notably, the significant pathways included metabolic pathways, carbon metabolism, the pentose phosphate pathway, the Foxo signaling pathway, and purine metabolism in the WR-II and WCC comparisons (Fig. 3F). In the WR-II and RCC comparison, the significantly enriched pathways were aminoacyl-tRNA biosynthesis; metabolic pathways; alanine, aspartate and glutamate metabolism; beta-alanine metabolism; and purine metabolism (Fig. 3G). These DMs were related mainly to metabolism, protein synthesis and development. Notably, the levels of fumaric acid, sphingosine, betaine and AMP in WR-II were significantly greater than those in WCC and RCC, and the four metabolites promoted host growth and development.

#### 3.4. Differential genes identification and functional enrichment

Transcriptome analysis of nine muscle samples from WR-II, WCC, and RCC yielded  $3.88 \times 10^8$  clean reads, with approximately 84.39 % mapped to the reference genome. Differentially expressed gene (DEG) analysis under stringent criteria revealed 5680 DEGs between WR-II and WCC, with 2694 upregulated DEGs and 2986 downregulated DEGs. A

**Table 2**Alpha diversity index of the gut bacterial communities of WR-II, WCC and RCC.

	•	•			
Sample	Goods_coverage	Observed_features	Chao1	Simpson	Shannon
WR-II	1.000	0.334	409.882	0.623	2.896
WCC	1.000	0.507	885.538	0.914	5.225
RCC	1.000	0.534	942.857	0.864	5.008

Note: n = 3.

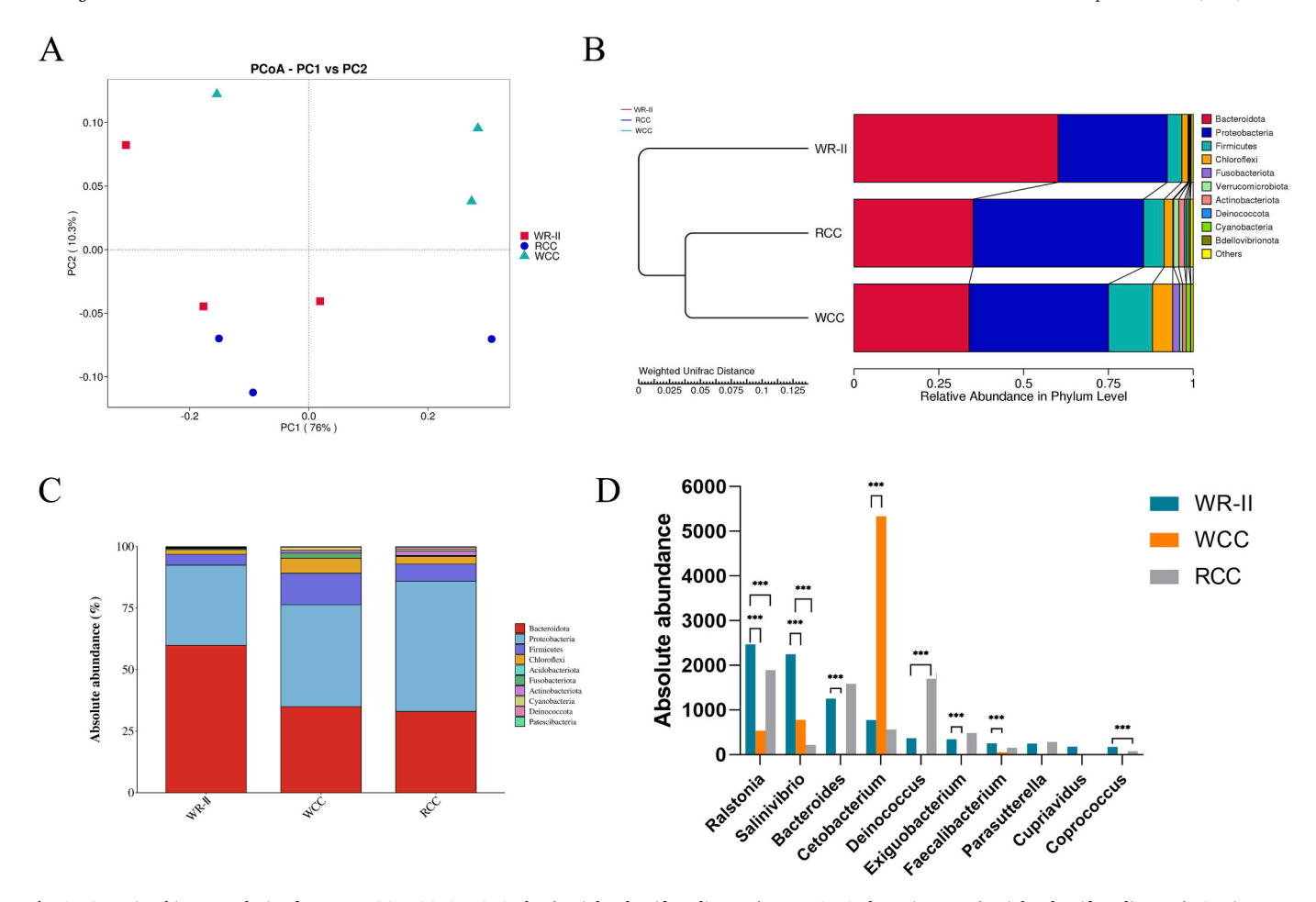


Fig. 2. Gut microbiome analysis of WR-II, WCC, RCC. A. PCoA plot (Weighted unifrac distance). B. UPGMA clustering tree (Weighted unifrac distance). C. Histogram of the top 10 absolute abundances of WR-II, WCC, and RCC intestinal bacterial phyla. D. Comparison of the WR-II probiotics top 10 with its parents WCC and RCC.

total of 11,795 genes were differentially expressed between WR-II and RCC, with 6064 upregulated and 5731 downregulated (Fig. 4A). KEGG enrichment analysis of the DEGs revealed that the pathways significantly enriched in the WR-II and WCC comparisons included oxidative phosphorylation, ribosome, focal adhesion, protein processing in the endoplasmic reticulum, and the citrate cycle (TCA cycle). In the WR-II and RCC comparison, the significantly enriched pathways were focal adhesion; mitophagy; the NOD-like receptor signaling pathway; autophagy; and valine, leucine and isoleucine degradation. These findings indicate that the DEGs, compared with those in WCC and RCC, are related mainly to protein synthesis and substance metabolism.

To verify the expression levels of the growth-related genes, the DEGs were annotated via GO functional analysis and KEGG enrichment analysis. Common growth-related terms identified in WR-II, WCC, and RCC included insulin-like growth factor binding (GO:0005520), response to growth factor (GO:0070848), insulin signaling pathway (KO 04910), FoxO signaling pathway (KO 04068), and the mTOR signaling pathway (KO 04150). Additionally, representative genes for these growth-related terms, including *irs1*, *akt*, *foxo1*, *igf1r*, and *irs2*, were more highly expressed in WR-II than in its parents, WCC and RCC (Table 3).

#### 3.5. Multi-omics correlation analysis

DMs and DEGs were mapped to KEGG pathway databases to identify shared pathways and determine the main biochemical and signal transduction pathways (Fig. 5). In the WR-II and WCC comparisons, the growth-related target pathways identified included the FoxO signaling pathway (3 metabolites, 72 transcripts), the mTOR signaling pathway (2

metabolites, 66 transcripts), oxidative phosphorylation (3 metabolites, 110 transcripts), and carbon metabolism (12 metabolites, 57 transcripts) (Fig. 5A). In the WR-II and RCC comparisons, the target pathways included the mTOR signaling pathway (2 metabolites, 144 transcripts), the FoxO signaling pathway (3 metabolites, 135 transcripts), carbon metabolism (3 metabolites, 135 transcripts), and oxidative phosphorylation (3 metabolites, 85 transcripts) (Fig. 5B).

To better understand the mechanism of action of the intestinal flora and its metabolites in promoting host growth, Pearson correlation analyses were performed on the basis of the above data, including intestinal probiotics (OTUs generated by 16S rDNA sequencing), intestinal metabolites (DMs enriched in the growth-related pathway), and growthrelated gene expression (DEGs enriched in the growth-related pathway). The results revealed that intestinal probiotics and DMs were significantly associated with the expression of growth-related genes (Fig. 5C). Ralstonia is positively correlated with DMs but does not meet the criteria for significance (p < 0.05). However, Salinivibrio was significantly positively correlated with AMP (r = 0.70, p < 0.05), fumaric acid (r =0.69, p < 0.05), ADP (r = 0.61, p < 0.05) and adenosine 5'-monophosphate (r = 0.64, p < 0.05) (Table S4). In addition, DMs and DEGs enriched in the same pathway were significantly correlated (Table S5). In the FoxO signaling pathway, AMP was significantly positively correlated with *irs1* (r = 0.85, p < 0.01), and *foxo1* (r = 0.79, p < 0.05). In the mTOR signaling pathway, AMP was significantly positively correlated with *irs1* (r = 0.85, p < 0.01). Multi-omics analysis revealed that in WR-II with rapid growth, the role of intestinal probiotics in muscle growth is related to the activation of the FoxO signaling pathway and the mTOR signaling pathway. Moreover, irs1 and foxo1 were identified as the main effectors, and AMP was identified as a potential

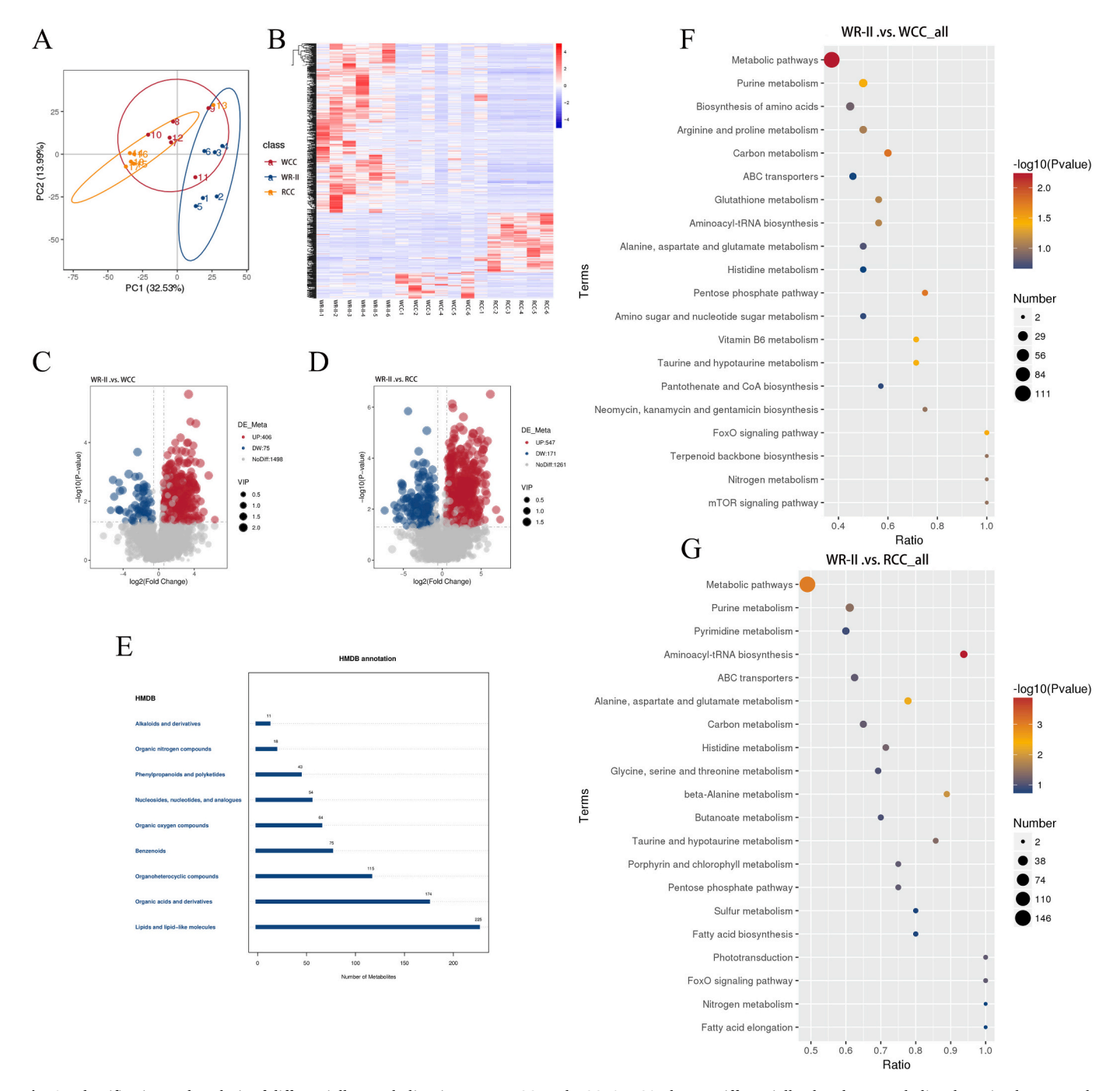


Fig. 3. Identification and analysis of differentially metabolites in WR-II, WCC, and RCC. A. PCA plot. B. Differentially abundant metabolite clustering heatmap; the vertical direction represents the clustering of samples, and the horizontal direction represents the clustering of metabolites. C, D Differentially abundant metabolite volcano map. E. Differentially abundant Metabolite HMDB classification statistical chart. F, G. Differentially abundant metabolite KEGG enrichment map.

messenger in the gut-muscle axis.

# 3.6. RT-PCR validation

To verify the reliability of the transcriptome data, we selected ten important genes, namely, Insulin receptor substrate 1 (*irs1*), Forkhead box O1 (*foxo1*), Insulin-like growth factor 1 (*igf1*), Growth hormone receptor (*ghr*), AKT serine/threonine kinase 1 (*akt1*), Mechanistic target of rapamycin complex 1 (*mtorc1*), Myostatin b (*mstnb*), myogenin (*moyg*), Myogenic differentiation antigen (*myod*) and Phosphoinositide 3-kinase (*pi3k*) of the growth-associated pathway for RT–qPCR validation. As shown in Fig. 6. The RT–qPCR results were consistent with the

transcriptome data, confirming the authenticity of the transcriptome sequence and validating its reliability. (See Fig. 6.)

# 4. Discussion

Fish constitute an essential food source. The growth rate of fish not only affects farming efficiency but also directly impacts the sustainability of the aquaculture industry (Vélez et al., 2017). Distant hybridization usually results in heterosis, which is reflected in a fast growth rate, high disease resistance and high nutritional content (Liu et al., 2018; Liu, 2010; Liu et al., 2016). In previous studies, WR-II, which has fast growth, high muscle protein content, and strong stress resistance

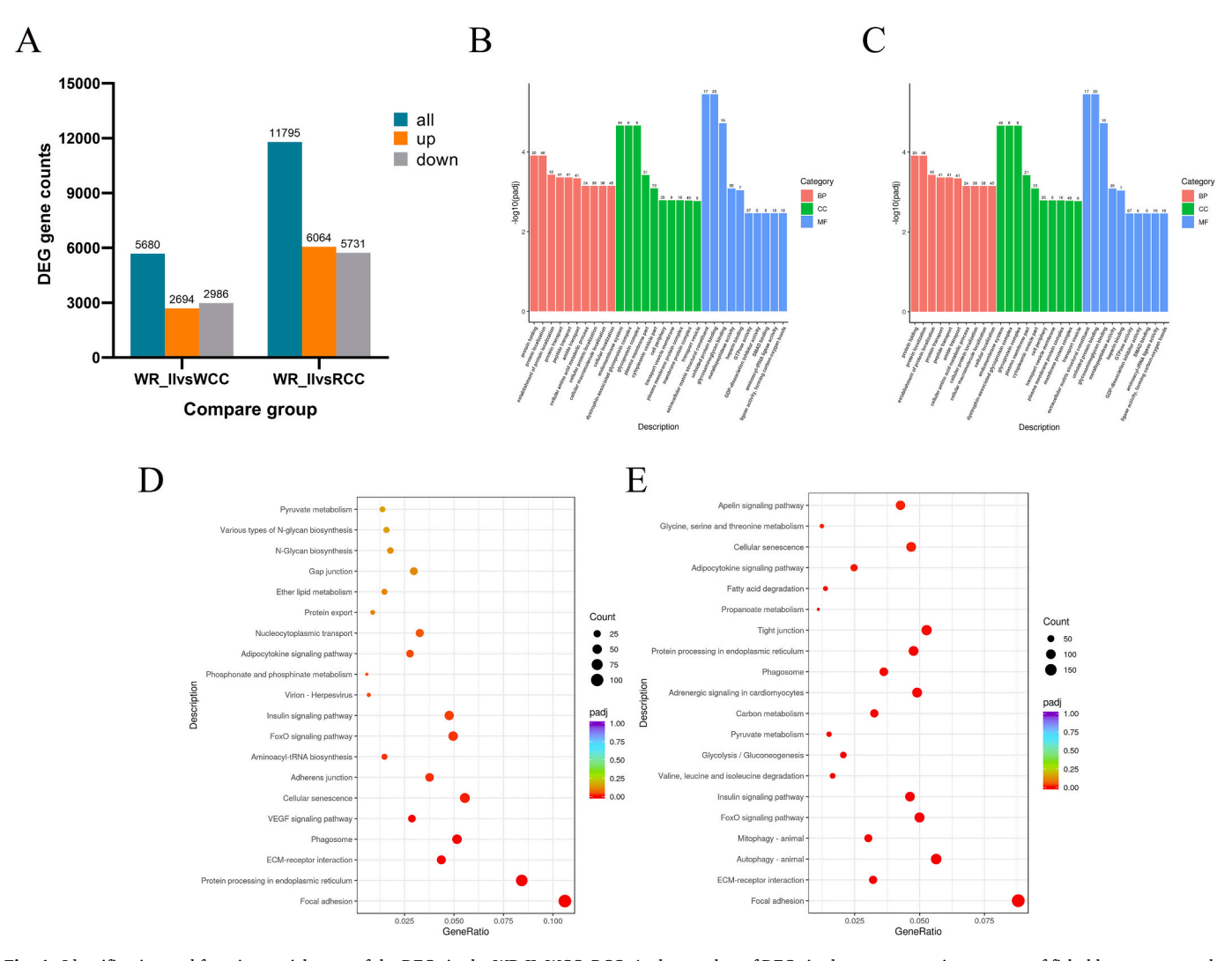


Fig. 4. Identification and function enrichment of the DEGs in the WR-II, WCC, RCC. A. the number of DEGs in the two comparison groups of fish: blue represents the total DEGs; yellow represents the upregulated genes; gray represents the downregulated genes. B, C. Upregulated differential gene GO functional enrichment analysis. D, E. KEGG enrichment analysis of the upregulated DEGs in two comparison groups. (For interpretation of the references to colour in this figure legend, the reader is referred to the web version of this article.)

**Table 3**Genes associated with growth shared among the sets of WR-II DEGs.

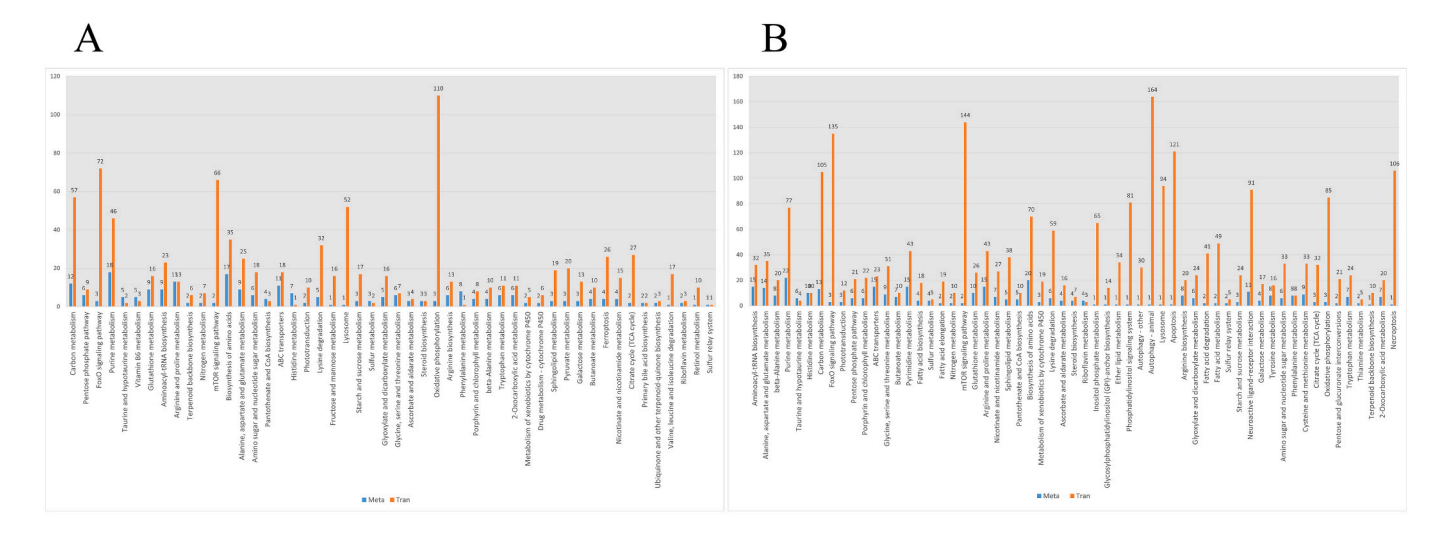
Gene	log2 (WR-II/WCC)	p value	log2 (WR-II/RCC)	p value
irs1	2.60	P < 0.01	6.99	P < 0.01
akt	1.53	P < 0.01	2.35	P < 0.01
foxo1	3.33	P < 0.01	5.35	P < 0.01
igf1r	2.59	P < 0.01	4.39	P < 0.01
irs2	3.17	P < 0.01	7.16	P < 0.01

Note: p < 0.01 indicates a extreme significant difference.

was obtained via distant hybridization (Liu et al., 2019; Zhang et al., 2024). The mucosa and submucosa form numerous intestinal folds within the intestinal lumen, and the number of these folds is positively correlated with the number of intestinal epithelial cells; more folds increase the absorptive capacity of the intestine (Morrison and Wright Jr, 1999; Verdile et al., 2020). Furthermore, goblet cells are critical indicators of the digestive and absorptive capabilities of the intestine. Studies have shown that these cells secrete various mucus substances, primarily neutral and acidic GCs, which play a significant role in the absorption process and the transport of macromolecules across membranes (Birchenough et al., 2015; Pelaseyed et al., 2014). In this study, WR-II had more intestinal folds, and the height, width and goblet cell

density of the intestinal folds were greater than those of its parents (Table 1). This result indicated that the digestion and absorption of WR-II were better than those of its parents, which may promote the rapid growth of WR-II. In addition, the greater number of intestinal folds of WR-II results in a large intestinal surface area that can accommodate more types of intestinal flora fixations, such as *Cupriavidus*, which is only found in WR-II (Fig. 2, D).

Many studies have confirmed the close relationship between the gut microbiota and host growth (Vargas-Albores et al., 2021). The stability, diversity, and abundance of the gut microbial community can influence fish growth rates (Su et al., 2021a). There are many probiotics in the vast gut flora, and probiotics are increasingly being recognized for their ability to positively alter the gut microbiota and improve metabolism (Falcinelli et al., 2018). In this study, the abundances of Ralstonia and Salinivibrio were significantly greater in the intestines of WR-II than in those of to its parents (Fig. 2, D). Ralstonia is highly abundant in the intestines of marine fish, with fewer reports in freshwater fish (Huang et al., 2020; Kim et al., 2007). In studies on the impact of algae on the gut microbiota of sea bream, Ralstonia exhibited antibacterial activity or the biosynthesis of bioactive compounds and may produce beneficial secondary metabolites for the host (Cerezo-Ortega et al., 2021). Salinivibrio promotes the production of extracellular proteins, polysaccharides or enzymes (Logan et al., 2006). In Salinivibrio species, research has found



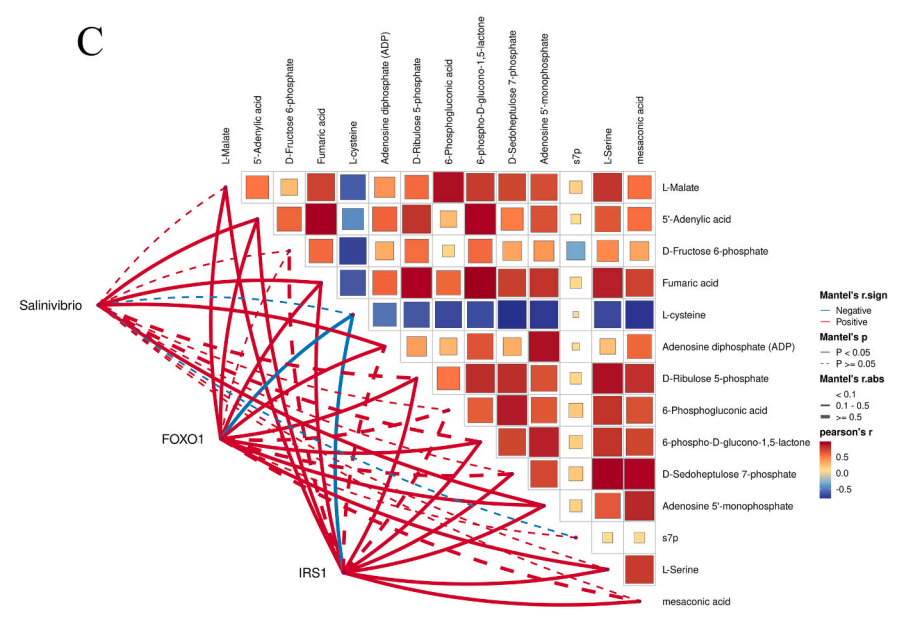


Fig. 5. Multi-omics analysis of WR-II, WCC and RCC. A, B DMs and DEGs were subjected to pathway enrichment analysis. C Multi-omics Pearson correlation analysis, the data derived from OTUs generated by 16 S rDNA sequencing, muscle RNA-Seq transcriptomics, and differential metabolites in the untargeted metabolomics.

that the ectABC-asp gene is present in all genomes, and members of the genus can biosynthesize ectoine using the enzyme encoded by ectABCasp, ectoine is essential for the growth of this species at low temperatures (de la Haba et al., 2019; Ongagna-Yhombi and Boyd, 2013). A recent genome mining study of Salinivibrio proteolyticus M318 described the presence of the TRAP TeaABC transporter and the operon doeABXCD for ectoine catabolism in this species (Van Thuoc et al., 2020). In addition, one of their most interesting applications includes the production of a novel type of restriction endonuclease (Galisteo et al., 2019). Cupriavidus is unique to WR-II compared with its parents and has been found to be involved in nitrogen fixation and nodule formation in legumes, as well as other plant growth-promoting activities (Gyaneshwar et al., 2011). Therefore, on the basis of reports in the literature and the abundance of Ralstonia, Salinivibrio and Cupriavidus in WR-II, we hypothesize that three probiotics have a growth-promoting effect on the growth of WR-II. In studies of the metabolome, growth-related DMs such as fumaric acid, sphingosine, betaine and 5'-adenylic acid (AMP) were identified (Fig. 3). Fumonisin can reduce the expression of igf1 and ghr mRNAs in fingerlings and juveniles by inhibiting the biosynthesis of sphingolipids via the inhibition of sphingosine kinase (da Silva et al., 2019). These findings suggest that sphingosine plays a role in fish growth. Betaine improves the growth of fish and is already used as a feed additive for fish (Clarke et al., 1994; Fredette et al., 2000; ÖZYURT and POLAT Özyurt and Polat, 2001). AMP plays a crucial role in various cellular metabolic processes by being interconverted to adenosine triphosphate (ATP) and adenosine diphosphate (ADP). Additionally, AMP functions allosterically, with some studies suggesting that it acts as both an allosteric regulator and a direct agonist for AMP-activated protein kinase (AMPK) (Gowans and Hardie, 2014; Jauker et al., 2015). The levels of these four metabolites in WR-II were significantly greater than those in its parents, which may promote the rapid growth of WR-II. Finally, in comparative transcriptome analyses, we identified terms with growth-related GO functions and KEGG enrichment analysis and identified several representative genes, among which irs1, akt, foxo1, igf1r, and irs2 were significantly upregulated (Table 3). In conclusion, we found evidence of fast growth of WR-II in terms of gut microbes, gut metabolites and gene expression.

With the development of high-throughput technology, Multi-omics analysis has been widely used in fish genetic breeding research, and has achieved many results in research fields such as genetic diversity (Kim and Kim, 2021), environmental adaptability (Wang et al., 2024; Wen et al., 2019), aquaculture improvement (Li et al., 2017), and

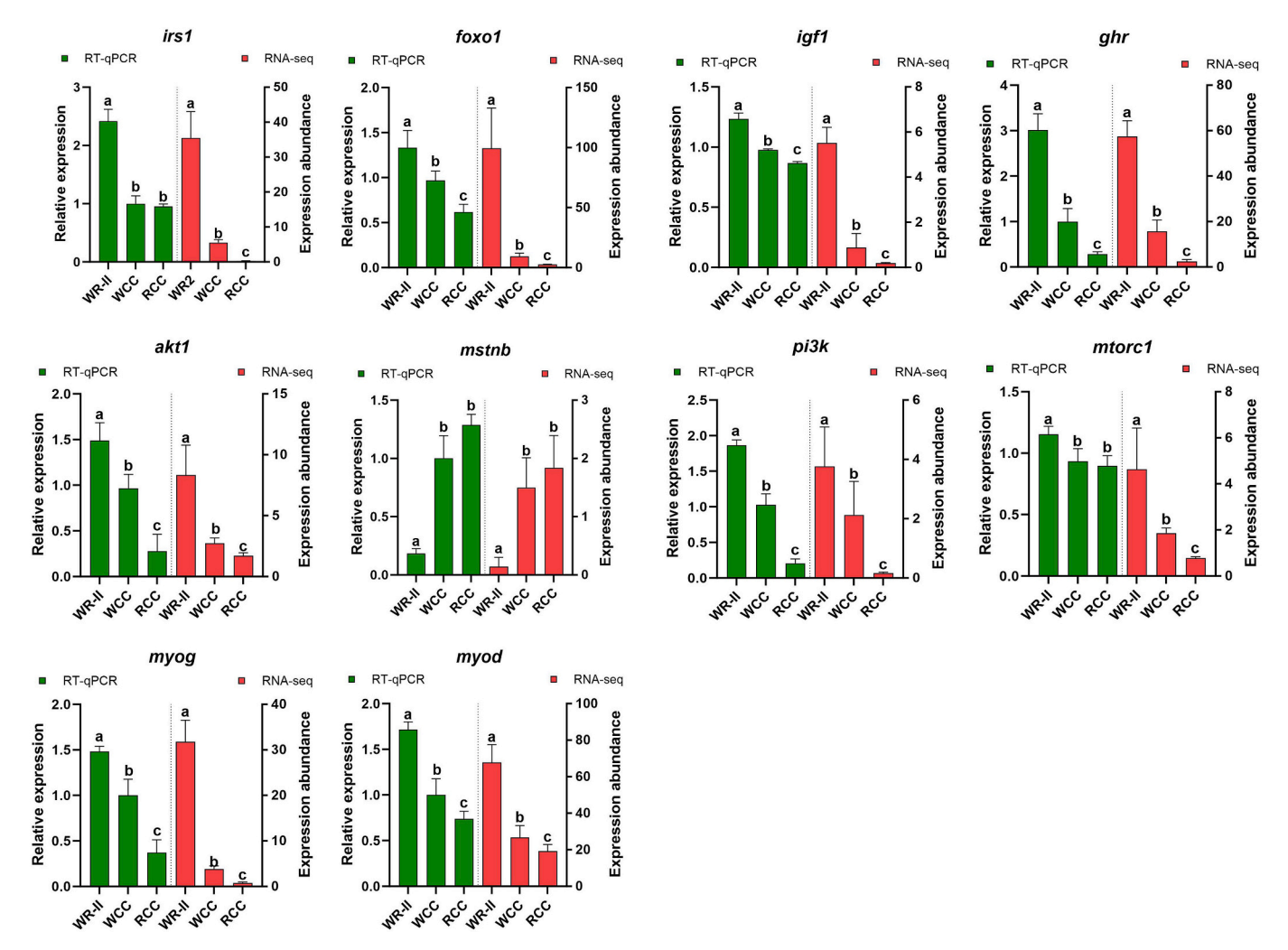
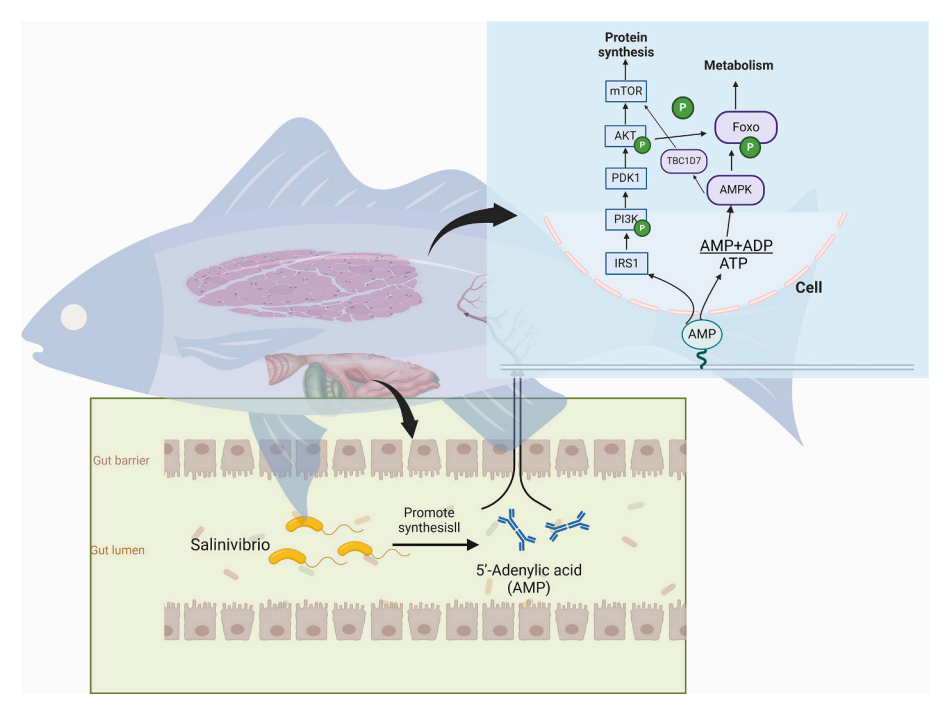


Fig. 6. The relative mRNA levels of key growth-related genes in RCC, WCC and WR-II were determined by RT-qPCR. Different lowercase letters indicate significant differences (*P* < 0.05).

disease control (He et al., 2021; Zhong et al., 2023). In this study, we revealed the molecular mechanisms involved in the rapid growth of hybrid fish via the integration of gut microbes, gut metabolomics, and muscle transcriptomics (Fig. 7). The gut microbiota synthesizes and regulates metabolites mainly from food-derived, nondigestible organic matter and endogenous secretions (Macfarlane and Macfarlane, 2002; Serino et al., 2009; Song et al., 2022). In this study, we found that the abundance of Salinivibrio and the level of AMP in the gut of WR-II were significantly greater than those in the gut of its parents, and the results revealed that Salinivibrio was significantly positively correlated with AMP (Fig. 5). Therefore, Salinivibrio may promote the production of AMP. Furthermore, small molecules present in the gut can traverse the intestinal barrier and enter the circulatory system, where they can promote or inhibit gene expression (Burcelin, 2016; Li et al., 2018; van der Knaap and Verrijzer, 2016). In this study, AMP was significantly positively correlated with irs1 and foxo1, which were enriched in both the mTOR signaling pathway and the FoxO signaling pathway (Fig. 5). AMPK regulates energy homeostasis by sensing the AMP + ADP/ATP ratio (Hardie, 2014; Hardie et al., 2006; Mihaylova and Shaw, 2011). AMPK signaling acts downstream to control a complex signaling network that includes the growth-related FoxO and mTOR signaling pathways (Burkewitz et al., 2014; Edwards et al., 2010; Martin-Montalvo et al.). AMPK regulates insulin receptors (IRs), particularly irs1, thereby controlling the insulin signaling pathway (Chopra et al., 2012). This pathway provides survival signals to cells by continuously activating protein kinase B (Akt) (Long et al., 2011). Studies have

demonstrated that *akt* activates the mTOR signaling pathway, which increases amino acid uptake and promotes protein synthesis (Bassel-Duby and Olson, 2006; Glass, 2003). *Akt* also phosphorylates and inactivates Foxo transcription factors, leading to a decreased expression of genes that promote muscle autophagy (Zhao et al., 2007). In this study, the expression of *irs1* increased, activating *akt* and thus the mTOR signaling pathway. Interestingly, the expression of *foxo1* also increased, which is contrary to the above results. However, studies have found that the upregulation of the *foxo1* can also stimulate cell proliferation (Liang et al., 2020). The precise mechanism remains under investigation. These results revealed an important pathway that can promote the rapid growth of WR-II. *Salinivibrio* can promote the production of the metabolite AMP, which activates the mTOR signaling pathway and the FoxO signaling pathway by upregulating *irs1* and *foxo1*.

In conclusion, this study provides a comprehensive view of the different profiles of the gut microbiota, gut metabolites and muscle transcriptome in improved fish from distant hybridization and its parents. Furthermore, the mechanism by which intestinal microbes and their metabolites promote the rapid growth of hybrid fish was identified through Multi-omics analysis. We propose that beneficial intestinal bacteria, particularly *Salinivibrio*, can increase the level of the metabolite AMP, which in turn promotes the expression of *irs1* and *foxo1*. Then, the mTOR and FoxO signaling pathways are activated. Our study demonstrated that the gut microbiota and its metabolites play a significant role in host growth and elucidated the molecular mechanism of fast growth in hybrid fish.



**Fig. 7.** Diagram of the mechanism of action of the intestinal muscle axis postulated in this experiment. The intestinal probiotic *Salinivibrio* from WR-II was able to regulate the level of 5′-adenylic acid, and AMP acted via transmembrane transport with the circulatory system to muscle cells, activating the FoxO1 gene in the FoxO signaling pathway and the IRS1 gene in the mTOR signaling pathway.

#### CRediT authorship contribution statement

Xuanyi Zhang: Writing – original draft. Fanglei Liu: Writing – review & editing. Bei Li: Data curation. Lujiao Duan: Data curation. Jianming Yu: Data curation. Ziyi Huang: Writing – review & editing. SiYang Huang: Writing – review & editing. Hongwen Liu: Writing – review & editing. Shaojun Liu: Writing – review & editing. Preview & editing. Shaojun Liu: Writing – review & editing.

## Declaration of competing interest

The authors declare that they have no known competing financial interests or personal relationships that could have appeared to influence the work reported in this paper.

#### Acknowledgments

This work was supported by the National Key Research and Development Program of China (2023YFD2400202), the National Natural Science Foundation of China (Grants No. 32002382, 32293252, and 32293254, U19A2040), the Training Program for Excellent Young Innovators of Changsha (Grant No. kq2200013), the Natural Science Foundation of Hunan Province (Grant No. 2021JJ40339), the Special Funds for Construction of Innovative Provinces in Hunan, the Earmarked Fund for Agriculture Research System of China (Grant No. CARS-45), the Laboratory of Lingnan Modern Agriculture Project (Grant No. NT2021008), the 111 Project (D20007), and Special Science Found of Nansha-South China Agricultural University Fishery Research Institute, Guangzhou.

# Appendix A. Supplementary data

Supplementary data to this article can be found online at https://doi.org/10.1016/j.aquaculture.2024.741783.

#### Data availability

The complete clean reads for these libraries have been uploaded to the NCBI Sequence Read Archive site (http://www.ncbi.nlm.nih.gov/sra/; Accession Nos. SRR25395549, SRR25395550, SRR25395553, SRR25395557, SRR25395558, SRR25395559, SRR29662862, SRR29662861, SRR29662860.)

#### References

Bassel-Duby, R., Olson, E.N., 2006. Signaling pathways in skeletal muscle remodeling. Annu. Rev. Biochem. 75 (1), 19–37.

Birchenough, G.M., Johansson, M.E., Gustafsson, J.K., Bergström, J.H., Hansson, G., 2015. New developments in goblet cell mucus secretion and function. Mucosal Immunol. 8 (4), 712–719.

Blanchard, J.L., Watson, R.A., Fulton, E.A., Cottrell, R.S., Nash, K.L., Bryndum-Buchholz, A., Büchner, M., Carozza, D.A., Cheung, W.W., Elliott, J., 2017. Linked sustainability challenges and trade-offs among fisheries, aquaculture and agriculture. Nature Ecology & Evolution 1 (9), 1240–1249.

Bokulich, N.A., Subramanian, S., Faith, J.J., Gevers, D., Gordon, J.I., Knight, R., Mills, D. A., Caporaso, J.G., 2013. Quality-filtering vastly improves diversity estimates from Illumina amplicon sequencing. Nat. Methods 10 (1), 57–59.

Burcelin, R., 2016. Gut microbiota and immune crosstalk in metabolic disease. Molecular metabolism 5 (9), 771–781.

Burkewitz, K., Zhang, Y., Mair, W.B., 2014. AMPK at the nexus of energetics and aging. Cell Metab. 20 (1), 10–25.

Cerezo-Ortega, I.M., Di Zeo-Sánchez, D., García-Márquez, J., Ruiz-Jarabo, I., Sáez-Casado, M., Balebona, M., Moriñigo, M., Tapia-Paniagua, S., 2021. Microbiota composition and intestinal integrity remain unaltered after the inclusion of hydrolysed Nannochloropsis gaditana in Sparus aurata diet. Sci. Rep. 11 (1), 18779.

Chen, S., Wen, J., Shuang, L., Xu, W., Xu, X., Zheng, G., Zou, S., 2023. Comparative analysis of the growth performance, histological structure and gut microbiota of F3 hybrids of blunt snout bream (Megalobrama amblycephala?)× topmouth culter (culter alburnus.). Aquaculture 574, 739727.

Chopra, I., Li, H., Wang, H., Webster, K., 2012. Phosphorylation of the insulin receptor by AMP-activated protein kinase (AMPK) promotes ligand-independent activation of the insulin signalling pathway in rodent muscle. Diabetologia 55, 783–794.

Cinar, K., Şenol, N., 2006. Histological and histochemical characterization of the mucosa of the digestive tract in flower fish (Pseudophoxinus antalyae). Anat. Histol. Embryol. 35 (3), 147–151.

Clarke, W.C., Virtanen, E., Blackburn, J., Higgs, D.A., 1994. Effects of a dietary betaine/ amino acid additive on growth and seawater adaptation in yearling Chinook salmon. Aquaculture 121 (1–3), 137–145.

da Silva, S.C.C., Lala, B., de Oliveira Carniatto, C.H., Schamber, C.R., Nascimento, C.S., Braccini, G.L., Porto, C., Roldi, G., Tanamati, F., Gasparino, E., 2019. Fumonisin

- affects performance and modulates the gene expression of IGF-1 and GHR in Nile tilapia fingerlings and juveniles. Aquaculture 507, 233–237.
- de la Haba, R.R., López-Hermoso, C., Sánchez-Porro, C., Konstantinidis, K.T., Ventosa, A., 2019. Comparative genomics and phylogenomic analysis of the genus Salinivibrio. Front. Microbiol. 10, 2104.
- Edwards, A.G., Donato, A.J., Lesniewski, L.A., Gioscia, R.A., Seals, D.R., Moore, R.L., 2010. Life-long caloric restriction elicits pronounced protection of the aged myocardium: a role for AMPK. Mech. Ageing Dev. 131 (11–12), 739–742.
- Falcinelli, S., Rodiles, A., Hatef, A., Picchietti, S., Cossignani, L., Merrifield, D.L., Unniappan, S., Carnevali, O., 2018. Influence of probiotics administration on gut microbiota core: a review on the effects on appetite control, glucose, and lipid metabolism. J. Clin. Gastroenterol. 52, S50–S56.
- Fredette, M., Batt, J., Castell, J., 2000. Feeding stimulant for juvenile winter flounders. N. Am. J. Aquac. 62 (2), 157–160.
- Fu, B., Ma, H., Yang, H., Zheng, M., Zhang, J., Li, Y., Du, Y., Wang, G., Tian, J., Zhang, K., 2024. Broad bean (Vicia faba L.) caused abnormal lipid metabolism in grass carp (Ctenopharyngodon idellus) liver: insight from the gut microbiota–liver axis. Food Frontiers.
- Fuentes, E.N., Valdés, J.A., Molina, A., Björnsson, B.T., 2013. Regulation of skeletal muscle growth in fish by the growth hormone–insulin-like growth factor system. Gen. Comp. Endocrinol. 192, 136–148.
- Galisteo, C., Sánchez-Porro, C., de la Haba, R.R., López-Hermoso, C., Fernández, A.B., Farias, M.E., Ventosa, A., 2019. Characterization of Salinivibrio socompensis sp. nov., a new halophilic bacterium isolated from the high-altitude hypersaline lake Socompa, Argentina. Microorganisms 7 (8), 241.
- Glass, D.J., 2003. Signalling pathways that mediate skeletal muscle hypertrophy and atrophy. Nat. Cell Biol. 5 (2), 87–90.
- Gong, D., Xu, L., Liu, Q., Wang, S., Wang, Y., Hu, F., Wu, C., Luo, K., Tang, C., Zhou, R., 2021. A new type of hybrid bream derived from a hybrid lineage of Megalobrama amblycephala (9)× Culter alburnus (3). Aquaculture 534, 736194.
- Gong, D., Tao, M., Xu, L., Hu, F., Wei, Z., Wang, S., Wang, Y., Liu, Q., Wu, C., Luo, K., 2022. An improved hybrid bream derived from a hybrid lineage of Megalobrama amblycephala (9)× Culter alburnus (3). Sci. China Life Sci. 1–9.
- Gowans, G.J., Hardie, D.G., 2014. AMPK: A Cellular Energy Sensor Primarily Regulated by AMP. Portland Press Ltd.
- Grosicki, G.J., Fielding, R.A., Lustgarten, M.S., 2018. Gut microbiota contribute to agerelated changes in skeletal muscle size, composition, and function: biological basis for a gut-muscle axis. Calcif. Tissue Int. 102, 433–442.
- Guo, H.-H., Zheng, G.-D., Wu, C.-B., Jiang, X.-Y., Zou, S.-M., 2018. Comparative analysis of the growth performance and intermuscular bone traits in F1 hybrids of black bream (Megalobrama terminalis)(Q)× topmouth culter (culter alburnus)(3). Aquaculture 492, 15–23.
- Gyaneshwar, P., Hirsch, A.M., Moulin, L., Chen, W.-M., Elliott, G.N., Bontemps, C., Estrada-de Los Santos, P., Gross, E., dos Reis Jr., F.B., Sprent, J.I., 2011. Legumenodulating betaproteobacteria: diversity, host range, and future prospects. Mol. Plant Microbe Interact. 24 (11), 1276–1288.
- Hardie, D.G., 2014. AMPK—sensing energy while talking to other signaling pathways. Cell Metab. 20 (6), 939–952.
- Hardie, D.G., Hawley, S.A., Scott, J.W., 2006. AMP-activated protein kinase–development of the energy sensor concept. J. Physiol. 574 (1), 7–15.
- He, L., Zhu, D., Liang, X., Li, Y., Liao, L., Yang, C., Huang, R., Zhu, Z., Wang, Y., 2021. Multi-omics sequencing provides insights into age-dependent susceptibility of grass carp (Ctenopharyngodon idellus) to reovirus. Front. Immunol. 12, 694965.
- Hu, F., Zhong, H., Wu, C., Wang, S., Guo, Z., Tao, M., Zhang, C., Gong, D., Gao, X., Tang, C., 2021. Development of fisheries in China. Reproduction and Breeding 1 (1), 64-79
- Huang, Q., Sham, R.C., Deng, Y., Mao, Y., Wang, C., Zhang, T., Leung, K.M., 2020. Diversity of gut microbiomes in marine fishes is shaped by host-related factors. Mol. Ecol. 29 (24), 5019–5034.
- Jauker, M., Griesser, H., Richert, C., 2015. Spontaneous formation of RNA strands, peptidyl RNA, and cofactors. Angew. Chem. Int. Ed. 54 (48), 14564–14569.
- Kim, D.-Y., Kim, J.-M., 2021. Multi-omics integration strategies for animal epigenetic studies—A review. Animal bioscience 34 (8), 1271.
- Kim, D.H., Brunt, J., Austin, B., 2007. Microbial diversity of intestinal contents and mucus in rainbow trout (Oncorhynchus mykiss). J. Appl. Microbiol. 102 (6), 1654–1664.
- Lahiri, S., Kim, H., Garcia-Perez, I., Reza, M.M., Martin, K.A., Kundu, P., Cox, L.M., Selkrig, J., Posma, J.M., Zhang, H., 2019. The gut microbiota influences skeletal muscle mass and function in mice. Sci. Transl. Med. 11 (502), eaan5662.
- Larsen, A.M., 2014. Studies on the Microbiota of Fishes and the Factors Influencing their Composition. Auburn University.
- Li, X., Yan, Q., Xie, S., Hu, W., Yu, Y., Hu, Z., 2013. Gut microbiota contributes to the growth of fast-growing transgenic common carp (Cyprinus carpio L.). PloS One 8 (5), e64577.
- Li, T., Long, M., Li, H., Gatesoupe, F.-J., Zhang, X., Zhang, Q., Feng, D., Li, A., 2017. Multi-omics analysis reveals a correlation between the host phylogeny, gut microbiota and metabolite profiles in cyprinid fishes. Front. Microbiol. 8, 454.
- Li, X., Egervari, G., Wang, Y., Berger, S.L., Lu, Z., 2018. Regulation of chromatin and gene expression by metabolic enzymes and metabolites. Nat. Rev. Mol. Cell Biol. 19 (9), 563–578.
- Li, S., Yang, X., Fan, S., Zhou, Z., Zhou, R., Wu, C., Gong, D., Wen, M., Wang, Y., Tao, M., 2022. Comparative analysis of muscle nutrient in two types of hybrid bream and native bream. Reproduction and Breeding 2 (3), 71–77.
- Li, H., Li, W., Su, J., Zhou, Z., Miao, Y., Tian, X., Tao, M., Zhang, C., Zhou, Y., Qin, Q., 2024. Integration of transcriptome and metabolome reveals molecular mechanisms

- responsive to cold stress in gynogenetic mrigal carp (Cirrhinus mrigala). Aquaculture  $579,\,740200.$
- Liang, C.-Y., Huang, Z.-G., Tang, Z.-Q., Xiao, X.-L., Zeng, J.-J., Feng, Z.-B., 2020. FOXO1 and hsa-microRNA-204-5p affect the biologic behavior of MDA-MB-231 breast cancer cells. Int. J. Clin. Exp. Pathol. 13 (5), 1146.
- Liu, S., 2010. Distant hybridization leads to different ploidy fishes. Sci. China Life Sci. 53, 416–425.
- Liu, S., Luo, J., Chai, J., Ren, L., Zhou, Y., Huang, F., Liu, X., Chen, Y., Zhang, C., Tao, M., 2016. Genomic incompatibilities in the diploid and tetraploid offspring of the goldfish× common carp cross. Proc. Natl. Acad. Sci. 113 (5), 1327–1332.
- Liu, Q., Qi, Y., Liang, Q., Xu, X., Hu, F., Wang, J., Xiao, J., Wang, S., Li, W., Tao, M., 2018. The chimeric genes in the hybrid lineage of Carassius auratus cuvieri (9)× Carassius auratus red var.(3). Sci. China Life Sci. 61, 1079–1089.
- Liu, Q., Liu, J., Liang, Q., Qi, Y., Tao, M., Zhang, C., Qin, Q., Zhao, R., Chen, B., Liu, S., 2019. A hybrid lineage derived from hybridization of Carassius cuvieri and Carassius auratus red var. and a new type of improved fish obtained by back-crossing. Aquaculture 505, 173–182.
- Liu, D., Ren, Y., Zhong, S., Xu, B., 2024. New insight into utilization of fish by-product proteins and their skin health promoting effects. Mar. Drugs 22 (5), 215.
- Logan, N.A., Lappin-Scott, H.M., Oyston, P.F., 2006. Prokaryotic Diversity: Mechanisms and Significance. Cambridge University Press.
- Long, Y.C., Cheng, Z., Copps, K.D., White, M.F., 2011. Insulin receptor substrates Irs1 and Irs2 coordinate skeletal muscle growth and metabolism via the Akt and AMPK pathways. Mol. Cell. Biol. 31 (3), 430–441.
- Lozupone, C.A., Stombaugh, J.I., Gordon, J.I., Jansson, J.K., Knight, R., 2012. Diversity, stability and resilience of the human gut microbiota. Nature 489 (7415), 220–230.
- Ma, N., Ma, X., 2019. Dietary amino acids and the gut-microbiome-immune axis: physiological metabolism and therapeutic prospects. Compr. Rev. Food Sci. Food Saf. 18 (1), 221–242.
- Ma, N., He, T., Johnston, L.J., Ma, X., 2020. Host-microbiome interactions: the aryl hydrocarbon receptor as a critical node in tryptophan metabolites to brain signaling. Gut Microbes 11 (5), 1203–1219.
- Macfarlane, G.T., Macfarlane, S., 2002. Diet and metabolism of the intestinal flora. Bioscience and Microflora 21 (4), 199–208.
- Mihaylova, M.M., Shaw, R.J., 2011. The AMPK signalling pathway coordinates cell growth, autophagy and metabolism. Nat. Cell Biol. 13 (9), 1016–1023.
- Minich, J.J., Petrus, S., Michael, J.D., Michael, T.P., Knight, R., Allen, E.E., 2020. Temporal, environmental, and biological drivers of the mucosal microbiome in a wild marine fish, Scomber japonicus. Msphere 5 (3). https://doi.org/10.1128/ msphere, 00401-00420.
- Morrison, C., Wright, J., 1999. RA study of the histology of the digestive tract of the Nile tilapia. J. Fish Biol. 54 (3), 597–606.
- Morrison, C., Wright Jr., J., 1999. A study of the histology of the digestive tract of the Nile tilapia. J. Fish Biol. 54 (3), 597–606.
- Neis, E.P., Dejong, C.H., Rensen, S.S., 2015. The role of microbial amino acid metabolism in host metabolism. Nutrients 7 (4), 2930–2946.
- Okamoto, T., Morino, K., Ugi, S., Nakagawa, F., Lemecha, M., Ida, S., Ohashi, N., Sato, D., Fujita, Y., Maegawa, H., 2019. Microbiome potentiates endurance exercise through intestinal acetate production. Am. J. Physiol. Endocrinol. Metab. 316 (5), E956–E966.
- Ongagna-Yhombi, S.Y., Boyd, E.F., 2013. Biosynthesis of the osmoprotectant ectoine, but not glycine betaine, is critical for survival of osmotically stressed Vibrio parahaemolyticus cells. Appl. Environ. Microbiol. 79 (16), 5038–5049.
- Özyurt, G., Polat, A., 2001. Effects of DL-alanine and betaine supplemented diets on the growth and body composition of fingerling rainbow trout (Oncorhynchus mykiss, W. 1972). Turkish Journal of Veterinary & Animal Sciences 25 (3), 301–307.
- Pelaseyed, T., Bergström, J.H., Gustafsson, J.K., Ermund, A., Birchenough, G.M., Schütte, A., van der Post, S., Svensson, F., Rodríguez-Piñeiro, A.M., Nyström, E.E., 2014. The mucus and mucins of the goblet cells and enterocytes provide the first defense line of the gastrointestinal tract and interact with the immune system. Immunol. Rev. 260 (1), 8–20.
- Polakof, S., Míguez, J., Soengas, J., 2011. Evidence for a Gut-Brain Axis Used by Glucagon-like Peptide-1 to Elicit Hyperglycaemia in Fish. J. Neuroendocrinol. 23 (6), 508–518.
- Reinecke, M., 2010. Influences of the environment on the endocrine and paracrine fish growth hormone–insulin-like growth factor-I system. J. Fish Biol. 76 (6), 1233–1254.
- Rohr, M.W., Narasimhulu, C.A., Rudeski-Rohr, T.A., Parthasarathy, S., 2020. Negative effects of a high-fat diet on intestinal permeability: a review. Adv. Nutr. 11 (1), 77–91.
- Roques, S., Deborde, C., Richard, N., Skiba-Cassy, S., Moing, A., Fauconneau, B., 2020. Metabolomics and fish nutrition: a review in the context of sustainable feed development. Rev. Aquac. 12 (1), 261–282.
- Rowland, I., Gibson, G., Heinken, A., Scott, K., Swann, J., Thiele, I., Tuohy, K., 2018. Gut microbiota functions: metabolism of nutrients and other food components. Eur. J. Nutr. 57, 1–24.
- Schug, H., Yue, Y., Fischer, S., Kortner, T.M., Schirmer, K., 2019. Time-and concentration-dependent expression of immune and barrier genes in the RTgutGC fish intestinal model following immune stimulation. Fish Shellfish Immunol. 88, 308–317.
- Serino, M., Luche, E., Chabo, C., Amar, J., Burcelin, R., 2009. Intestinal microflora and metabolic diseases. Diabetes Metab. 35 (4), 262–272.
- Song, X., Wang, L., Liu, Y., Zhang, X., Weng, P., Liu, L., Zhang, R., Wu, Z., 2022. The gut microbiota-brain axis: role of the gut microbial metabolites of dietary food in obesity. Food Res. Int. 153, 110971.
- Sparagon, W.J., Gentry, E.C., Minich, J.J., Vollbrecht, L., Laurens, L.M., Allen, E.E., Sims, N.A., Dorrestein, P.C., Kelly, L.W., Nelson, C.E., 2022. Fine scale transitions of

- the microbiota and metabolome along the gastrointestinal tract of herbivorous fishes. Animal Microbiome 4 (1), 33.
- Su, S., Jing, X., Zhang, C., Hou, Y., Li, Z., Yang, X., Xu, P., Zhu, J., 2021a. Interaction between the intestinal microbial community and transcriptome profile in common carp (Cyprinus carpio L.). Front. Microbiol. 12, 659602.
- Su, S., Jing, X., Zhang, C., Hou, Y., Li, Z., Yang, X., Zhou, X., Xu, P., Tang, Y., Zhu, J., 2021b. Interaction between the intestinal microbial community and transcriptome profile in common carp (Cyprinus carpio L.). Front. Microbiol. 12, 659602.
- van der Knaap, J.A., Verrijzer, C.P., 2016. Undercover: gene control by metabolites and metabolic enzymes. Genes Dev. 30 (21), 2345–2369.
- Van Thuoc, D., Loan, T.T., Trung, T.A., Van Quyen, N., Tung, Q.N., Tien, P.Q., Sudesh, K., 2020. Genome mining reveals the biosynthetic pathways of polyhydroxyalkanoate and ectoines of the halophilic strain Salinivibrio proteolyticus M318 isolated from fermented shrimp paste. Marine Biotechnol. 22, 651–660.
- Vargas-Albores, F., Martínez-Córdova, L.R., Hernández-Mendoza, A., Cicala, F., Lago-Lestón, A., Martínez-Porchas, M., 2021. Therapeutic modulation of fish gut microbiota, a feasible strategy for aquaculture? Aquaculture 544, 737050.
- Vélez, E., Lutfi, E., Azizi, S., Perelló, M., Salmerón, C., Riera-Codina, M., Ibarz, A., Fernández-Borràs, J., Blasco, J., Capilla, E., 2017. Understanding fish muscle growth regulation to optimize aquaculture production. Aquaculture 467, 28–40.
- Verdile, N., Pasquariello, R., Scolari, M., Scirè, G., Brevini, T.A., Gandolfi, F., 2020. A detailed study of rainbow trout (Onchorhynchus mykiss) intestine revealed that digestive and absorptive functions are not linearly distributed along its length. Animals 10 (4), 745.
- Wang, J., Xiao, J., Zeng, M., Xu, K., Tao, M., Zhang, C., Duan, W., Liu, W., Luo, K., Liu, Y., 2015. Genomic variation in the hybrids of white crucian carp and red crucian carp: evidence from ribosomal DNA. Sci. China Life Sci. 58, 590–601.
- Wang, S., Xu, X., Luo, K., Liu, Q., Chen, L., Wei, Z., Zhou, P., Hu, F., Liu, Z., Tao, M., 2020. Two new types of triploid hybrids derived from Cyprinus carpio (Q)× Megalobrama amblycephala (3). Aquaculture 528, 735448.
- Wang, Y., Guo, H., Gao, X., Wang, J., 2021. The intratumor microbiota signatures associate with subtype, tumor stage, and survival status of esophageal carcinoma. Front. Oncol. 11, 754788.

- Wang, M., Zhao, S., Wang, J., Nie, L., Li, L., Zhu, X., Zhang, L., 2024. Multi-omics analysis provides insight into liver metabolism in yellow catfish (Pelteobagrus fulvidraco) under hypoxic stress. Aquaculture 583, 740531.
- Want, E.J., Masson, P., Michopoulos, F., Wilson, I.D., Theodoridis, G., Plumb, R.S., Shockcor, J., Loftus, N., Holmes, E., Nicholson, J.K., 2013. Global metabolic profiling of animal and human tissues via UPLC-MS. Nat. Protoc. 8 (1), 17–32.
- Wen, X., Hu, Y., Zhang, X., Wei, X., Wang, T., Yin, S., 2019. Integrated application of multi-omics provides insights into cold stress responses in pufferfish Takifugu fasciatus. BMC Genomics 20, 1–15.
- Xu, Y., Tan, Q., Kong, F., Yu, H., Zhu, Y., Yao, J., Azm, F.R.A., 2019. Fish growth in response to different feeding regimes and the related molecular mechanism on the changes in skeletal muscle growth in grass carp (Ctenopharyngodon idellus). Aquaculture 512, 734295.
- Yan, H., Yu, B., Degroote, J., Spranghers, T., Van Noten, N., Majdeddin, M., Van Poucke, M., Peelman, L., De Vrieze, J., Boon, N., 2020. Antibiotic affects the gut microbiota composition and expression of genes related to lipid metabolism and myofiber types in skeletal muscle of piglets. BMC Vet. Res. 16, 1–12.
- Zhan, H., Xiong, Y., Wang, Z., Dong, W., Zhou, Q., Xie, S., Li, X., Zhao, S., Ma, Y., 2022. Integrative analysis of transcriptomic and metabolomic profiles reveal the complex molecular regulatory network of meat quality in Enshi black pigs. Meat Sci. 183, 108642
- Zhang, W., Li, F., Nie, L., 2010. Integrating multiple 'omics' analysis for microbial biology: application and methodologies. Microbiology 156 (2), 287–301.
- Zhang, X., Liu, F., Bei, L., Yu, J., Duan, L., Huang, Z., Zhou, Z., Shu, Y., Lin, J., Xiong, X., Liu, Q., Liu, S., 2024. Comparative analysis of nutrients in muscle and ovary between an improved fish and its parents. Reproduction and Breeding 4 (1), 16–21. https://doi.org/10.1016/j.repbre.2023.12.002.
- Zhao, J., Brault, J.J., Schild, A., Cao, P., Sandri, M., Schiaffino, S., Lecker, S.H., Goldberg, A.L., 2007. FoxO3 coordinately activates protein degradation by the autophagic/lysosomal and proteasomal pathways in atrophying muscle cells. Cell Metab. 6 (6), 472–483.
- Zhong, L., Liu, S., Zuo, F., Geng, Y., Ouyang, P., Chen, D., Yang, S., Zheng, W., Xiong, Y., Cai, W., 2023. The IL17 signaling pathway: a potential signaling pathway mediating gill hyperplasia and inflammation under ammonia nitrogen stress was identified by multi-omics analysis. Sci. Total Environ. 867, 161581.